

Chapter 3

Molecular Dynamics Simulations of Unbound, Agonist-Bound, and Inverse-Agonist-Bound Turkey $\beta 1$

3.1 Overview

As structural data for GPCRs become more readily available, the primary focus of GPCR research has shifted towards the mechanism of activation. It is believed that GPCRs exist in equilibrium between active and inactive states, even in the absence of ligand, and that ligand binding occurs through a series of incremental steps that eventually stabilize one form of the receptor.^{57,98} Drug development for GPCRs focuses by necessity on the “snapshot” perspective provided by X-ray crystal structures and predicted binding site structures, but the variety of conformations accessible to a target GPCR or family of targets complicates this design process. While the majority of GPCR-targeting drugs are antagonists or inverse agonists, a deeper understanding of the activation mechanism and its effect on the binding site can assist the development of agonist drugs to turn on rather than

shut down a specific receptor. In studying this problem with molecular dynamics (MD), we consider the movements of conserved regions thought to be important to activation or stabilization.

The role of the highly conserved D/ERY motif at the intracellular side of TM3 has been the subject of debate since the release of the β adrenergic and human adenosine receptors. In the bovine rhodopsin crystal structure, this triplet interacts with a conserved glutamate at the intracellular side of TM6, and is believed to function as an “ionic lock” that partially stabilizes an inactive form of the receptor. The β_2 , β_1 , and adenosine A_{2a} crystal structures lack this interaction, which may imply the ionic lock is not a conserved interaction. However, the long, flexible IC3 connecting TM6 to TM7 is treated differently in each crystal structure depending on what strategy was used to successfully crystallize the protein. It may be difficult, then to draw conclusions about the base of TM6 as its behavior and interactions may be governed by the presence (or absence) of IC3 and the associated G-protein. Fluorescence studies of human β_2 do show evidence for an ionic lock interaction that is disrupted upon activation by all but the weakest agonists, even though this interaction is not observed in the crystal structure.²⁵ For this debate, MD can offer an opportunity to explore the stability of these interactions in the presence of a complete IC3 loop and bound ligands as well as explicit solvent.

Class A GPCRs also share a conserved WXPFF motif in the center of TM6 that affects both ligand binding and receptor activation. The orientation of the Trp in this motif has been implicated as an early step in activation, as it shifts from

a “vertical” orientation with the aromatic sidechain parallel to the TM helix to a “horizontal” orientation perpendicular to TM6.⁹⁹ Yao, *et al.* illustrated the role of this rotation for $\beta 2$ occurring for full agonists and strong partial agonists.²⁵ In all available crystal structures, Trp^{6.48} is observed in the vertical, inactive orientation. A recent computational study of bovine rhodopsin also showed motion of this tryptophan “toggle switch” as well as involvement of the ionic lock and TM helix motions.¹⁰⁰

While motions of TM6 seem highly likely to play a role in activation, TM5 may also play a role that has only recently been explored. The crystal structure of active rhodopsin³² as well as the squid opsin structure¹⁰¹ show the TM5 helix elongated past the lipid membrane, an important difference between the active and inactive structures. Secondary structure predictions of several GPCRs, including the adrenergic receptors, show the possibility of this helix being extended. A virtual ligand screening study found that shifting TM5 of the human $\beta 2$ structure inwards towards the binding pocket improved predicted agonist binding, another possible link between TM5 movement and activation.¹⁰² Mutations of TM5 in rhodopsin affect activation by disrupting possible interactions with TM3.^{103–105} The predicted helical region of turkey $\beta 1$ contains several charged residues that can interact with either TM3 or TM6 to form an alternative ionic lock, but the precise nature of this helix’s contribution to activation remains unknown.

Some GPCRs are naturally constitutively active, showing second messenger activity even in the absence of ligand.⁴⁴ This complicates crystallization but allows

for easy study of ligand effects and GPCR deorphanization.¹⁰⁶ Systems with less constitutive activity have been engineered for study purposes, providing further insight into which parts of the TM bundle play a significant role in activation. Mutations in TMs 3 and 7 of the AT1 receptor create a constitutively active mutant.¹⁰⁷ Active mutants of $\beta 2$,¹⁰⁸ histamine H2,¹⁰⁹ and $\alpha 1b$ ²⁶ receptors result from mutation of the highly conserved DRY motif at the intracellular end of TM3. Mutations in TM6 cause constitutive activation for the rat μ opioid receptor,¹¹⁰ the $\alpha 1b$ adrenergic receptor,¹¹¹ and bovine rhodopsin.¹¹² One site in IC3 close to the beginning of TM6 also produces a constitutively active form of $\alpha 1b$.¹¹³ Additionally, Rasmussen *et al.* discovered activating mutations in the DRY motif of $\beta 2$ also caused a counterclockwise rotation of TM6.¹⁰⁸ It is clear that TM6 plays a role in the transition between active and inactive states, but TMs 3 and 7 likely also play a role.

The challenges posed by the dynamic behavior of GPCRs have led some researchers to explore stabilizing mutations in an effort to shut down GPCR activation and create a less dynamic, more easily crystallized receptor. The best stabilizing mutations for turkey $\beta 1$ described in Chapter 2 occur in TMs 2, 5, and 7 as well as two intracellular loops (IC1 joining TMs 1 and 2, and IC3 joining TMs 5 and 6). Joining the intracellular ends of TMs 3 and 6 results in an inactive form of rhodopsin.¹¹⁴ Recently, a stabilized variation of the leukotriene B_4 receptor BLT1 was engineered by including a metal binding site to connect the intracellular ends of TMs 3 and 6.⁴³ The common helices for both activating and stabilizing mutations are nearly always TMs 3 and 6, especially the conserved D/ERY motif in

TM3. These changes usually do not affect ligand binding dramatically, except that the stabilizing mutations may decrease agonist affinity in accord with the ternary complex model.

To test the role of ligand effects in these possible conformation changes in turkey $\beta 1$, MD with a variety of ligands can be performed and the resulting motions analyzed. As a receptor with little constitutive activity, $\beta 1$ offers an opportunity to observe the transition to an active state. Although inactive, the $\beta 1$ crystal structure does not contain the putative ionic lock. This interaction as well as the missing intracellular loop, can be built in for MD studies. Through 10 ns MD of the apo, inverse agonist bound, and agonist bound structures, we can observe the motions of TM helices that begin the process of GPCR activation.

3.2 Methods

NVT Langevin dynamics were carried out using NAMD¹¹⁵ and the CHARMM force field.⁹³ The complete systems include about 38,000 atoms each, including water. The SHAKE algorithm was used to prevent drift from fast modes.¹¹⁶ The bath temperature was set to 310K, and a Particle Mesh Ewald (PME) grid was used to calculate long-range interactions. For both minimization and equilibration, femtosecond timesteps were used. Before analysis, all frames were aligned to the last frame to minimize noise from structural drift.

The 2VT4 crystal structure⁴¹ served as the starting point for this study. The crystal ligand was removed, as were the crystal ions and other accompanying

molecules with the exception of the cyanopindolol ligand and the seven crystal waters. This structure was minimized, then the IC3 loop modeled with PLOP.^{117,118} This loop was built in 20-residue sections, beginning with the 10 residues at the intracellular ends of TMs 5 and 6, then the 10 residues attached to those, and so on until the entire loop was built and connected. The last seven residues of IC3 are found to be helical by the APSSP2 secondary structure prediction method,¹¹⁹ so the helical constraints available in PLOP were used to build these residues as an α helix. In order to test the role of Arg139^{3.50} and Glu285^{6.30} in stabilizing the receptor through an ionic lock, this interaction was built using SCREAM.⁹⁰ This modified receptor was minimized for 1,000 steps, ions were added, then it was placed into lipid (palmitoylcholine) and water (TIP3) and the lipid/water minimized for 5,000 steps and equilibrated for 0.5 ns. This entire system was minimized for 5,000 steps, then equilibrated for 10 ns. Figure 3.1 shows the energy fluctuations for the system after 6,000 steps.

The initially optimized receptor-solvent system became the foundation for ligand dynamics, both inverse agonist and agonist. The protein after initial optimization, but before the 10 ns equilibration, was modified to accommodate either the inverse agonist cyanopindolol or the agonist isoproterenol. For cyanopindolol, the crystal orientation of the ligand was merged with the optimized apo protein. The binding site, then the entire protein, was minimized for 5,000 steps. This system was then equilibrated for 10 ns. We predicted the agonist orientation using GenMSCDock in a procedure similar to that described in Chapter 4. Rather than

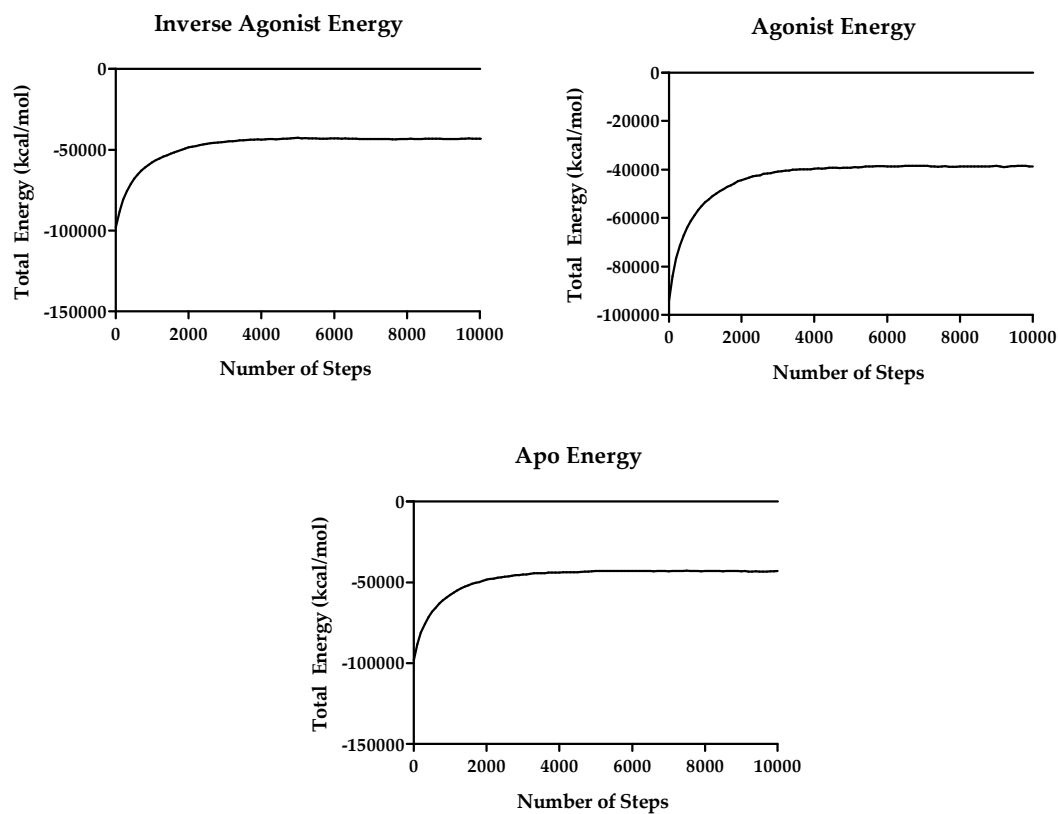


Figure 3.1: All three simulations reached a stable energy within the first 10 ps of the simulation, with the isoproterenol bound structure higher in energy, on average, than the apo or cyanopindolol bound structures.

DarwinDock, MSCDock based on USCF Dock 4¹²⁰ generated the docked poses using diversity and voronoi clustering, but the final optimization of the structures was similar. While both epinephrine and norepinephrine were docked, the best structure by energy that agreed with general adrenergic mutation data was a norepinephrine structure. This structure was converted to isoproterenol, a potent β selective agonist. Isoproterenol binds $\beta 1$ more tightly than do the endogenous agonists, and activates the receptor more quickly.¹²¹ Once built, this ligand was merged with the equilibrated apo protein and initial positions for the crystallographic waters, then optimized similarly to the cyanopindolol case. In both cases, energy fluctuations subsided within the first 10 ps of the simulation, shown in Figure 3.1.

3.3 Results and Discussion

Overall, the ligand bound structures shifted more than the apo protein. The RMSD over 10 ns changed less for unbound structure than for the ligand bound structures, as the ligand bound structures moved towards either an active or an inactive conformation (Figure 3.2). The ionic lock also does not move significantly over the course of the simulation, with a heavy-atom distance between Arg139^{3.50} and Glu285^{6.30} stable around 4 Å. This interaction does break in the last 2 ns of the apo simulation, as Arg275^{6.20} begins to interact with Glu285^{6.30} (illustrated in Figure 3.3). The lock does remain stable in the ligand-bound simulations, however, indicating that the lock interaction is relatively stable and that the competing residues

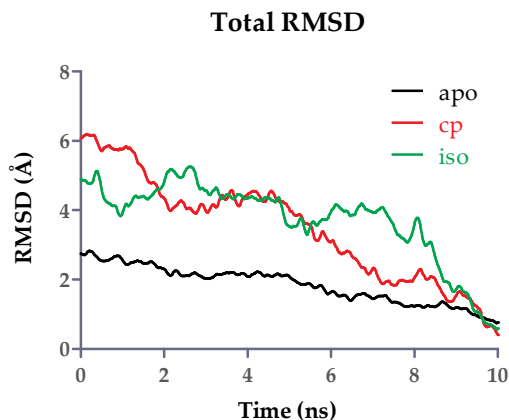


Figure 3.2: Total protein root-mean squared deviation is shown for all three MD simulations: apo protein in black, cyanopindolol (cp) bound in red, and isoproterenol (iso) bound in green. The apo protein moves the least, while the ligand bound forms move slightly more as they begin motion towards either a completely active or inactive conformation.

on IC3 are less likely to form a stable interaction due to the flexibility of the loop when ligand is present. The ionic lock distances are shown in Figure 3.4.

The TM6 toggle, Trp303^{6,48}, also does not shift significantly during the simulation (Figure 3.5). In $\beta 2$ simulations in the Goddard group, this residue does move, while the ionic lock remains stable over the 50 ns of that simulation. This system differs from $\beta 2$ in that turkey $\beta 1$ has less constitutive activity than $\beta 2$; this may indicate that the inactive state is considerably more stable for turkey $\beta 1$ than for $\beta 2$. The hallmarks of activation may not occur until later in the activation process for this receptor.

The beginning of the receptor-wide conformational change as illustrated here occurs with small movements of the TM helices themselves shifting towards or away from each other depending on the ligand involved. For the apo protein, the helices move relatively little. After about 7 ns of isoproterenol-bound dynamics,

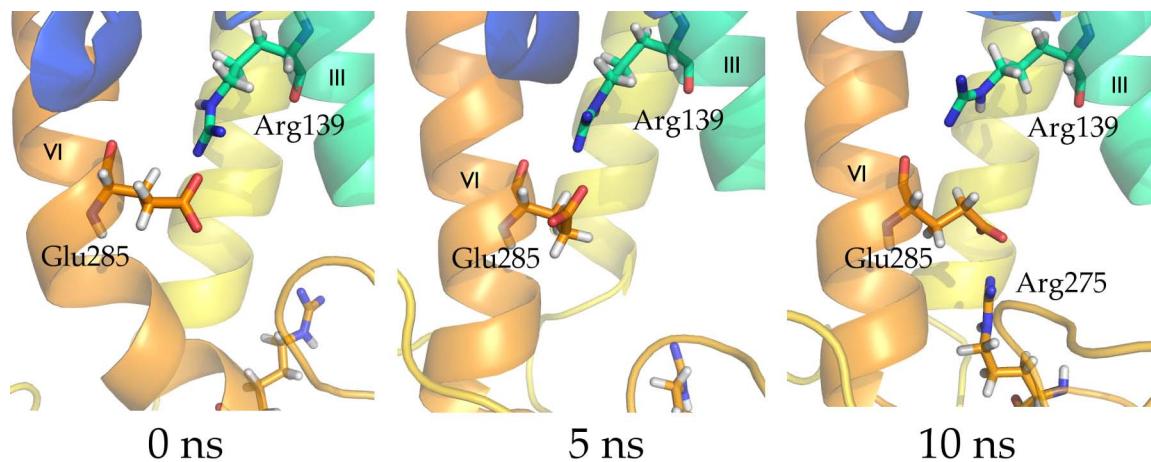


Figure 3.3: Although stable in the ligand bound simulations, the TM3-6 ionic lock breaks during 10 ns MD of the apo protein. In the last 2 ns, Arg275^{6.20} in the third intracellular loop shifts towards TM6 and interacts with Glu285^{6.30}

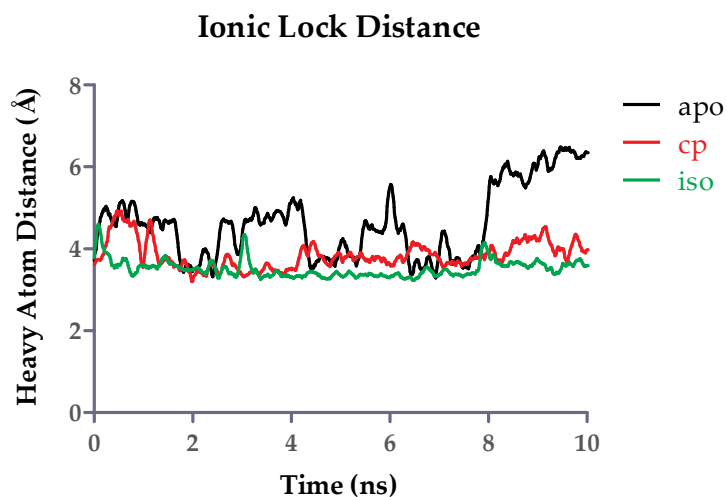


Figure 3.4: The ionic lock distance does not change significantly during the course of ligand-bound MD. At the end of the apo protein simulation, a residue from IC3 shifts to interact with Glu285^{6.30}, disrupting the ionic lock. Further studies will probe the stability of this interaction with alternate conformations of the receptor.

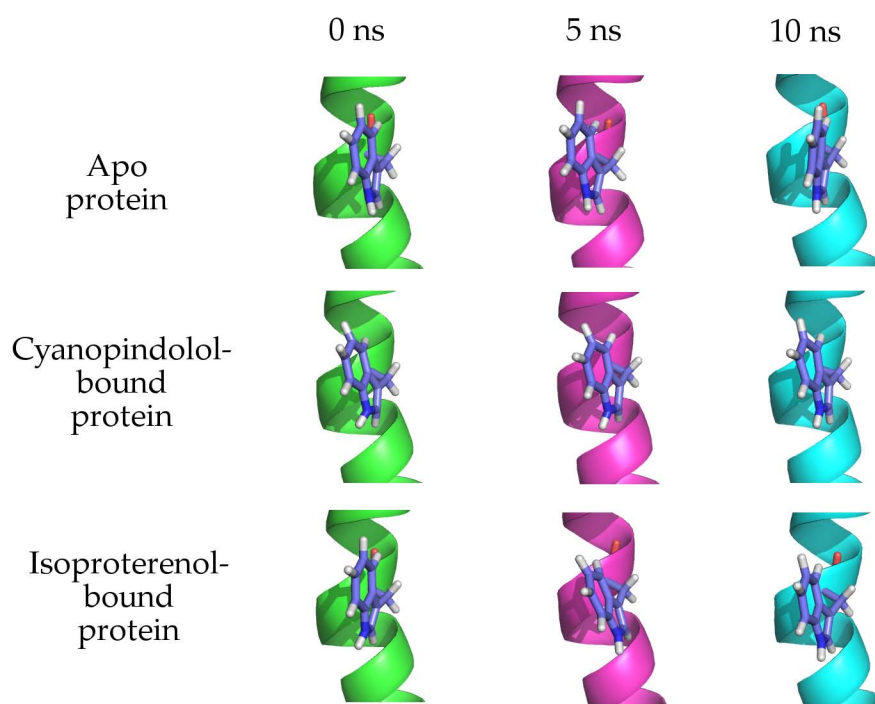


Figure 3.5: Although the residue fluctuates slightly, the 90° switch from the vertical rotamer of Trp303^{6,48} shown here and the horizontal rotamer thought to signify an activated state is not observed during the course of this study.

however, the total RMSDs of TMs 3, 5, and 6 begin to shift (Figure 3.6). Measuring the distance between the C and N termini of the TM helices gives a clearer sense of the helix motions involved. Figure 3.7 shows the distances between the tops of TMs 5 and 6, the bottoms of TMs 3 and 6, and the tops of TMs 1 and 7. The tops of TMs 5 and 6 move away from each other slightly in the apo and agonist bound forms, but towards each other as the inverse agonist binds. This is accompanied by a smaller inward shift by the intracellular ends of TMs 5 and 6. If the intracellular end of TM5 converts to a longer α helix extending into the cytosol, this inward movement may signify an alternate ionic lock between TMs 5 and 6 replacing the interaction between TMs 3 and 6.

As TM5 moves towards TM6, TM3 also shifts with respect to TM6. The distance between the intracellular ends of TMs 3 and 6, shown in Figure 3.7, indicates a trend towards breaking the ionic lock for the activated case (in green) and stabilizing it for the inactive case (in red). The distance fluctuates for the apo case, perhaps indicating the region is flexible. It may also be sensitive to the presence of G protein, which is not considered in this study. As the ionic lock only breaks in the last 2 ns of the apo simulation and not at all in the ligand-bound cases, this helix motion is likely the very beginning of the motion that eventually breaks the ionic lock and continues towards activation rather than the lock releasing the helices to move. These motions can also be seen in the changes to θ (defined as helix tilt angle, illustrated in Figure 3.9) over the course of the simulation. While the apo protein holds θ for the TM5 generally constant, TM5 in the isoproterenol-bound

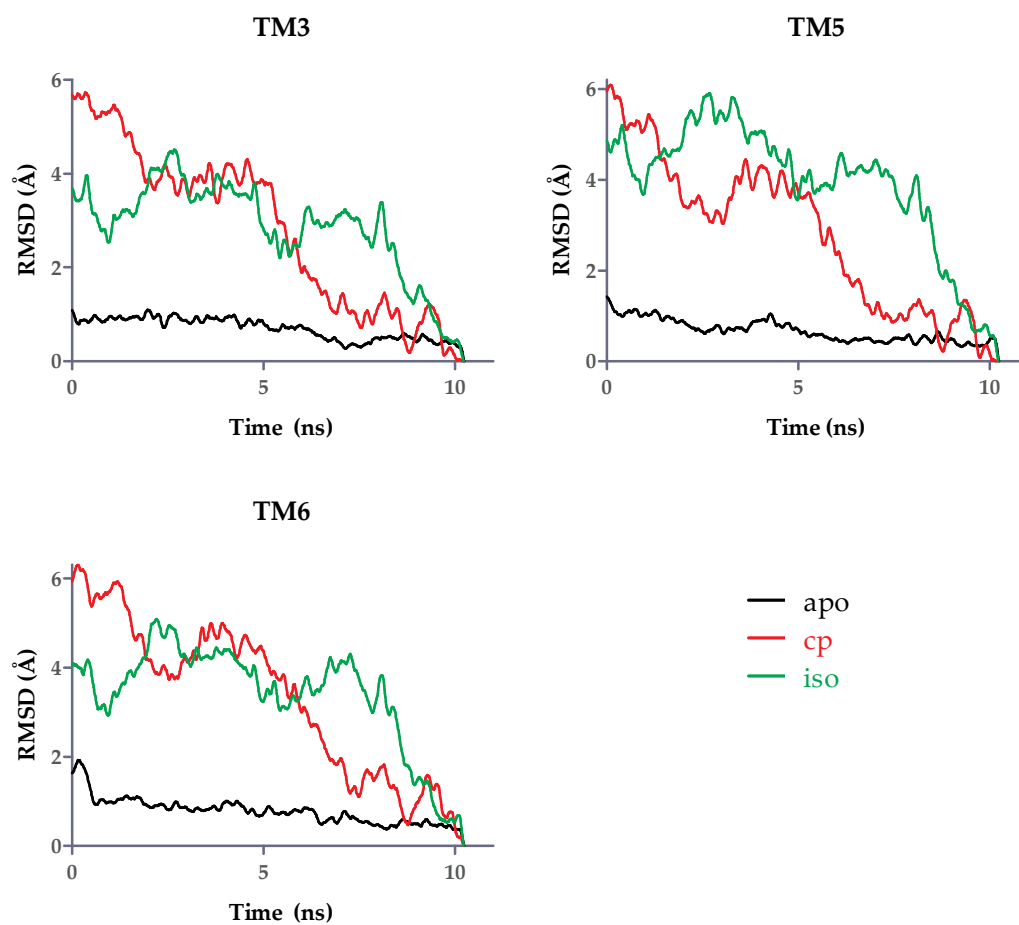


Figure 3.6: While the apo protein remains relatively still over the 10 ns of equilibration, the isoproterenol-bound system begins to diverge after 7 ns.

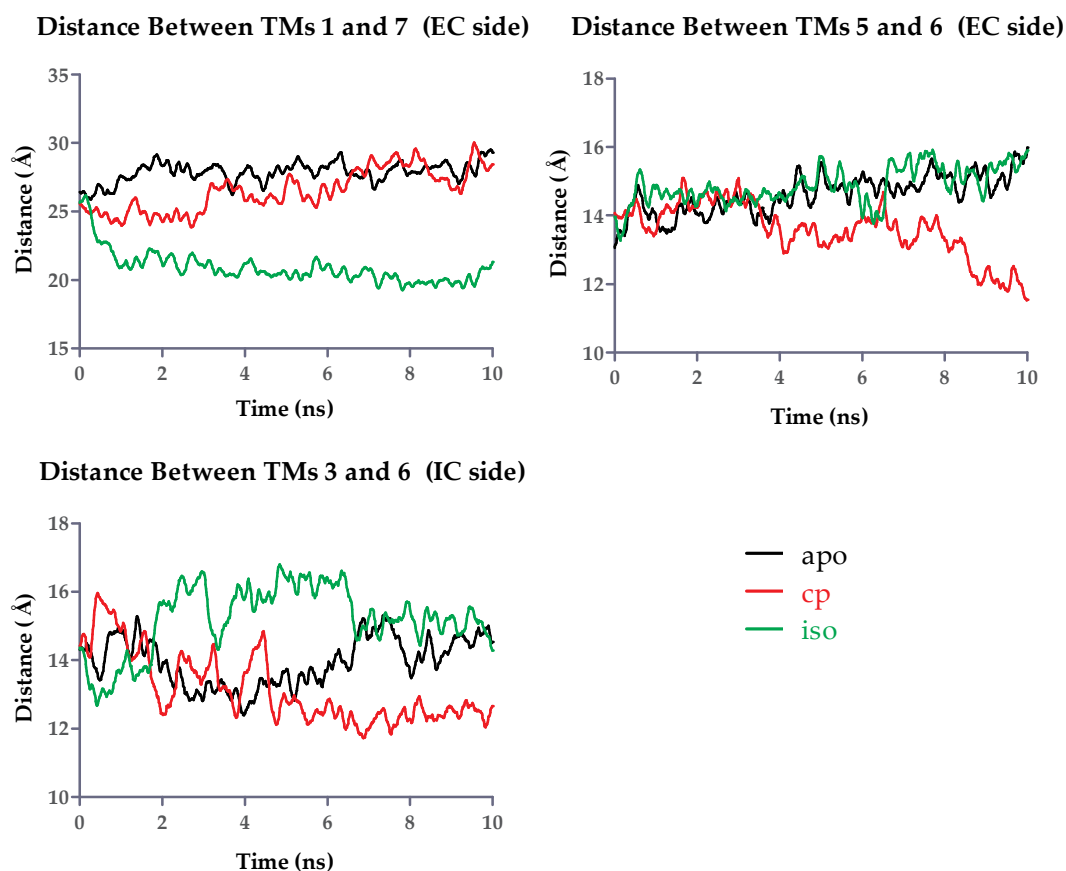


Figure 3.7: Distances between $C\alpha$ of the first or last residues of TMs 3, 5, 6, 1, and 7. These show the degree to which the ends of the helices are moving towards or away from one another, depending on the ligand bound. Inverse agonist binding causes the intracellular ends of TMs 3 and 6 and the extracellular ends of TMs 5 and 6 to move closer, while agonist binding causes TM1 to move closer to TM7.

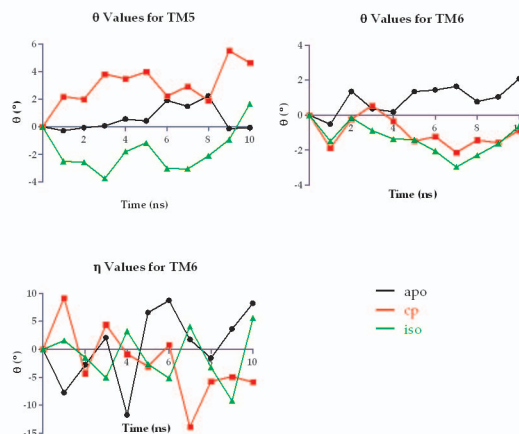


Figure 3.8: The changes in η for TM5 compared to TM6 reveal the closing of the distance between the intracellular ends of TMs 5 and 6 is due more to helix tilting for TM5 than any concerted motion by TM6. With ligand bound, (green and red) the rotation fluctuates but does not move decisively in one direction when the ligand is bound.

structure tilts “back,” moving the intracellular side in towards the TM bundle, a motion that is mirrored in the cyanopindolol-bound structure. TM6, on the other hand, is flexible but there is no strong trend towards tilting in one direction or another. While η rotation of TM6 has been implicated in receptor activation (shown in Figure 3.8), the overall helix rotation fluctuates and does not show a dramatic, concerted change. These results suggest the motion of surrounding helices initiate the transition, allowing TM6 to rotate later during activation.

An additional helix motion is observed over the course of this simulation: the intracellular end of TM1 moves slightly towards TM7 and remains close in the agonist bound case. For the apo and inverse agonist cases, the distances remain constant for most of the simulation and increase a small amount. The areas of contact between the two TMs are primarily hydrophobic, as the conserved Asn339^{7.49} is not positioned to interact with Asn59^{1.50}. This interaction could be tested ex-

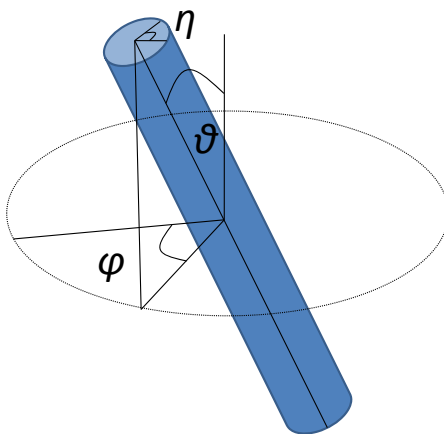


Figure 3.9: Decomposition of helix rotations produces three rotational modes: η , the rotation of the helix about the helical axis; θ , the helical tilt; and ϕ , the sweep angle of the helix.

perimentally by mutating some of these hydrophobic residues to polar ones to encourage TM1 to remain close to TM7 and facilitate activation of the system. Val62^{1.53} is positioned close to Tyr343^{7.53}, the conserved tyrosine in the NPXXY motif. If Val62^{1.53} is mutated to a polar or negatively charged residue, it might strengthen the interaction between the two helices. In addition, as Tyr^{7.53} is conserved throughout Class A GPCRs, this may be a general interaction useful for a variety of systems.

The $\beta 1$ crystal structure contains seven water molecules in the receptor structure, illustrated in Figure 3.10. Three of these remain stable during the isoproterenol simulation: one in the EC3 loop halfway between the extracellular ends of TMs 6 and 7, one in the EC1 loop close to TM2, and one associated with the NPXXY motif in TM7. Two of these remain stable during the apo protein simulation, the ones closest to TM7. Only the water associated with the NPXXY motif stays relatively fixed throughout the cyanopindolol simulation. It mediates the interaction

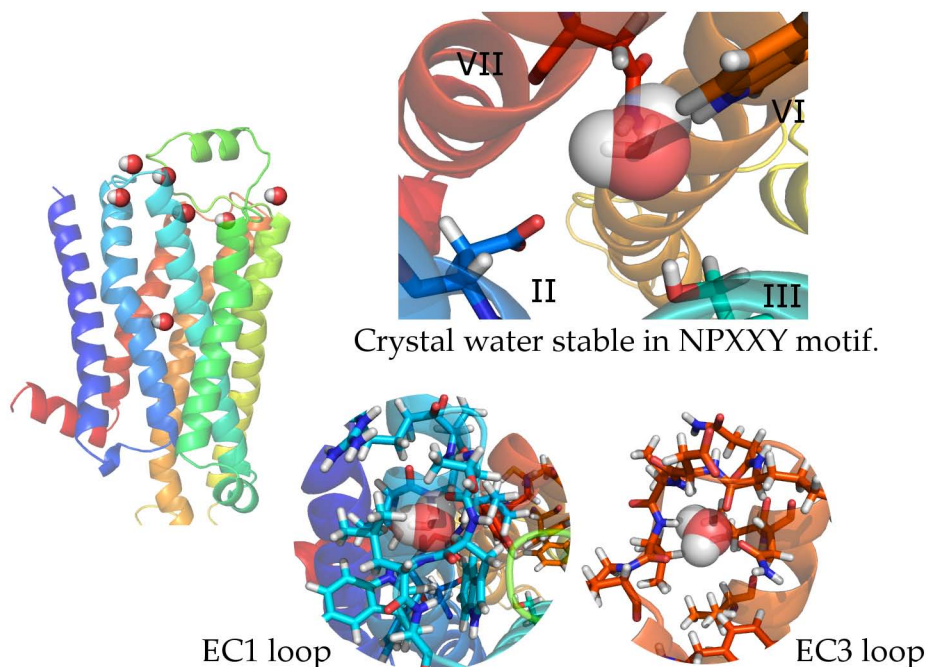


Figure 3.10: The crystal water stable in the NPXXY motif is shown in the upper right, with the conserved Asn335^{7.49} and Asp87^{2.50} holding it in place. The apo protein simulation shows the water associated with the EC3 loop, shown in the bottom right, is also stable. The EC1 loop water in the center bottom remains associated with the loop through the isoproterenol-bound simulation only. All seven crystal waters are illustrated at left.

between the conserved residues Asp87^{2.50} and Asn335^{7.49}, a region associated with ion regulation in $\alpha 2a$ ²¹ and universally conserved in Class A GPCRs. It is possible this is an ion binding site and the crystal water for this case is an ion responsible for stabilizing the TM2-7 interaction.

3.4 Conclusion

MD analysis of the turkey $\beta 1$ crystal structure reveals changes towards an equilibrated apo protein and helical shifts during the first 10 ns of full activation or deactivation. TMs 1, 3, and 5 move dramatically differently based on whether the

inverse agonist or full agonist is bound, but the hallmarks of activation involving TM6 do not begin during the 10 ns studied. TMs 1, 3, and 5 must therefore move in order to allow TM6 to rotate and change its conformation for full receptor activation.

The motion of TM1 towards TM7 upon agonist binding indicates a strengthened interaction between these helices that may contribute to constitutive activation. A mutation to TM1 to tether the helix to a conserved polar residue on TM7 may be useful in creating constitutively active mutants of orphan receptors for the purposes of identifying a native ligand. It may also stabilize an active state of the receptor enough to allow crystallization and X-ray characterization of an active form.

This study covered the very beginning steps of $\beta 1$ activation, and highlighted the movements of TMs 3, 6, and 5 that initiate the transition of the receptor from the inactive to the active state. The agonist equilibrated structure provides another starting point for further investigation into activation. With modifications to this equilibrated structure such as elongating the TM5 α -helix, creating an alternate salt bridge between TM5 and 6, and rotating Trp303^{6,48} to the active conformation, another MD simulation may illuminate which of these changes is stable in an active conformation and more likely to contribute to receptor activation.

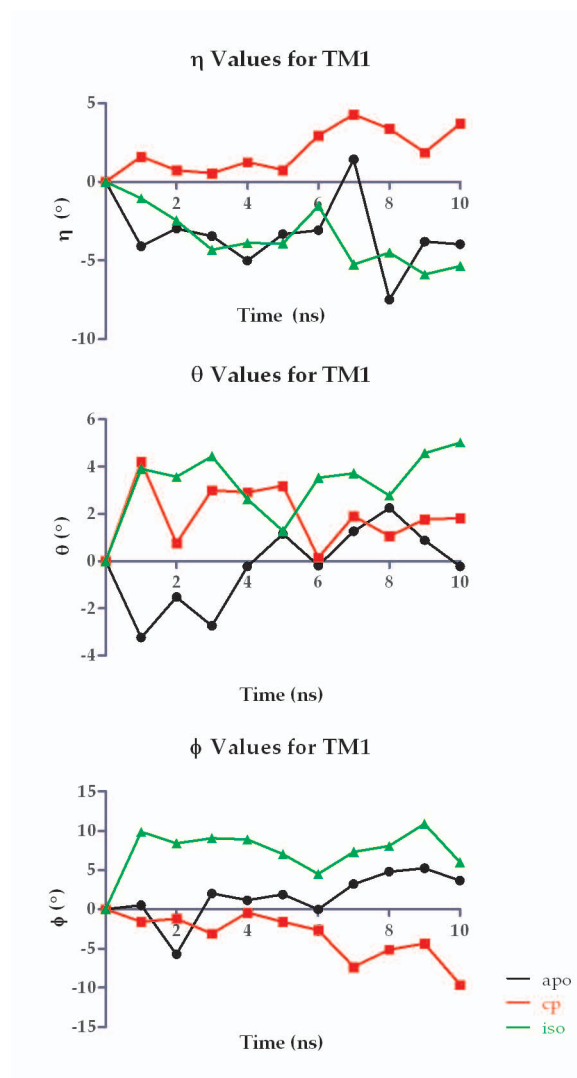


Figure 3.11: Changes to η , θ , and ϕ for TM 1 over the course of 10 ns full-solvent dynamics.

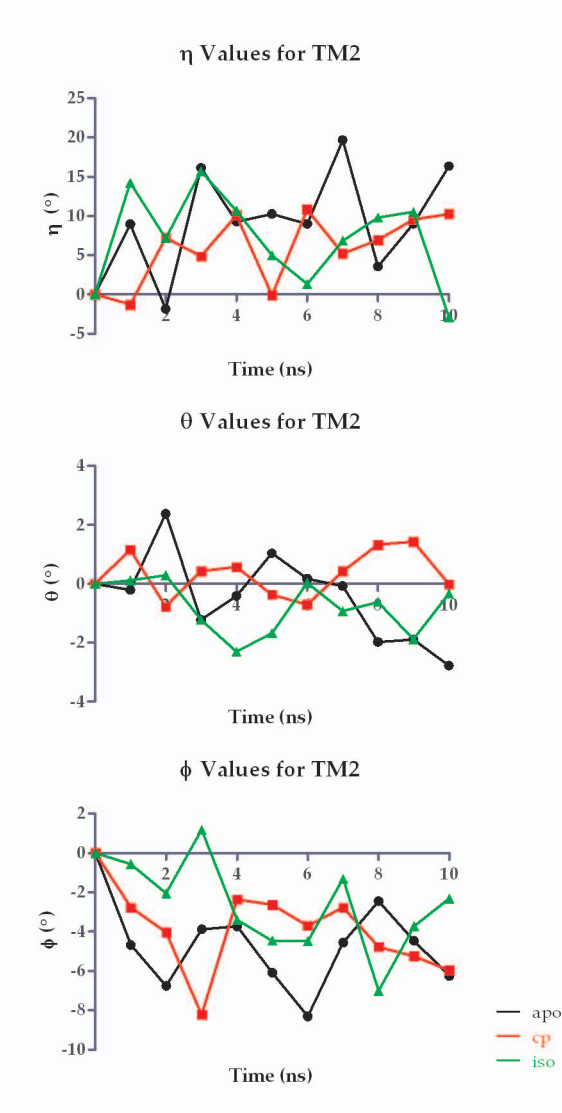


Figure 3.12: Changes to η , θ , and ϕ for TM 2 over the course of 10 ns full-solvent dynamics.

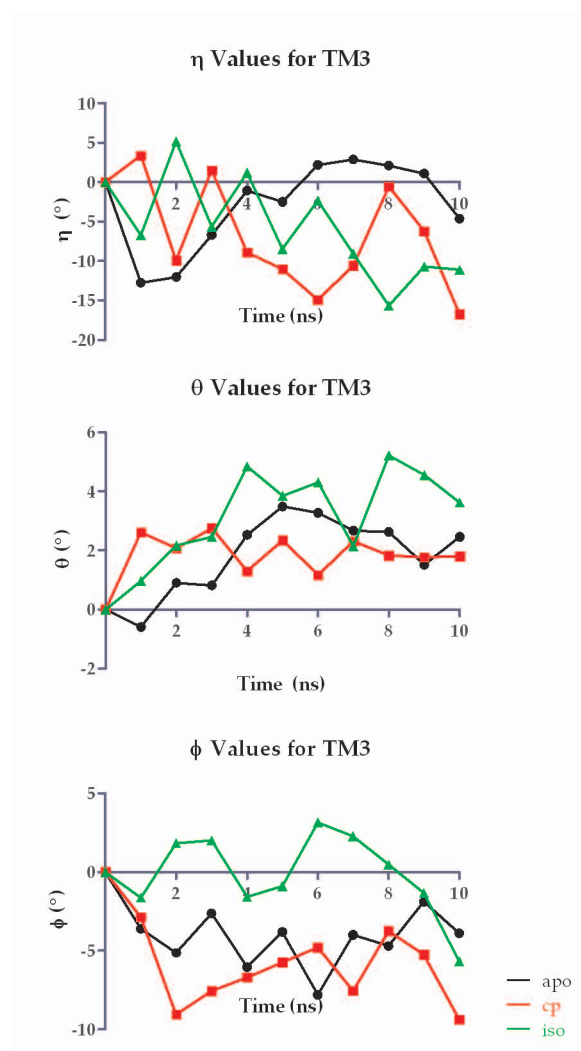


Figure 3.13: Changes to η , θ , and ϕ for TM 3 over the course of 10 ns full-solvent dynamics.

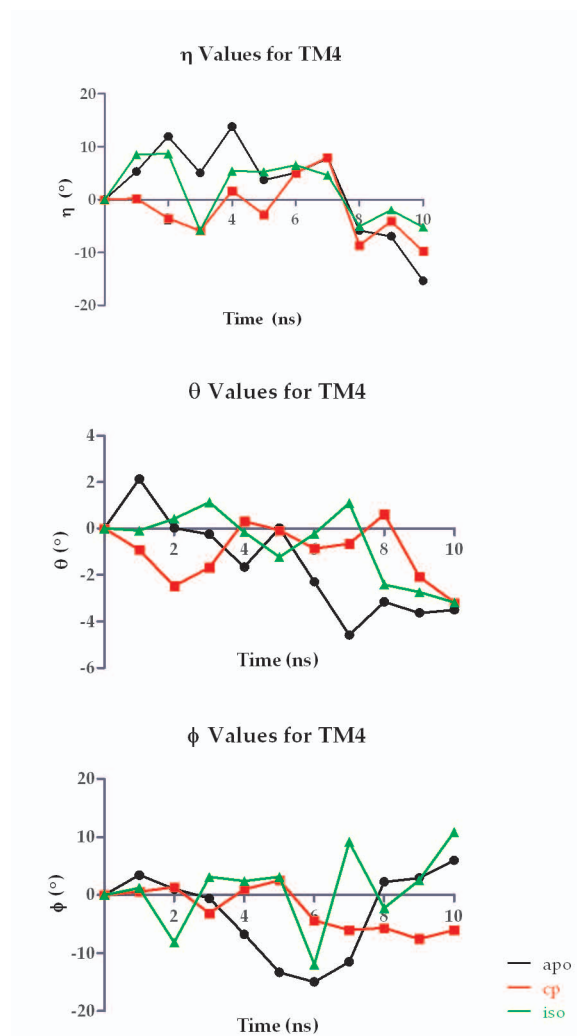


Figure 3.14: Changes to η , θ , and ϕ for TM 4 over the course of 10 ns full-solvent dynamics.

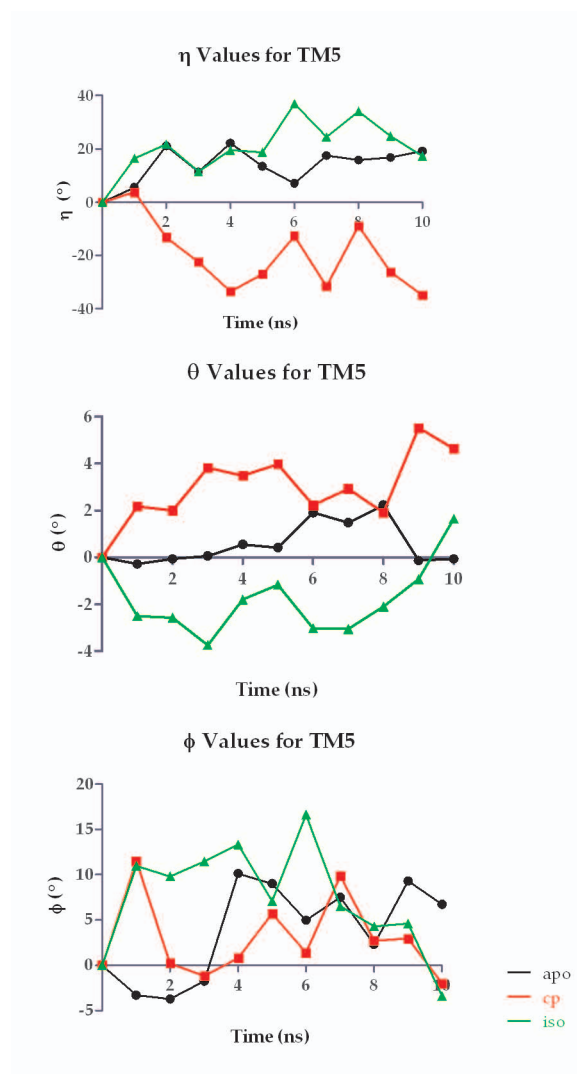


Figure 3.15: Changes to η , θ , and ϕ for TM 5 over the course of 10 ns full-solvent dynamics.

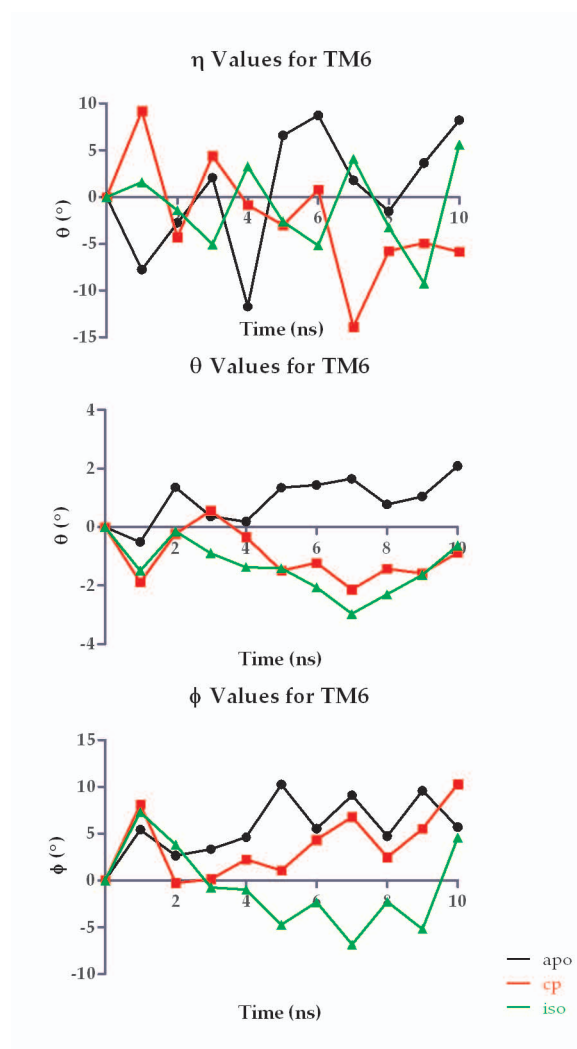


Figure 3.16: Changes to η , θ , and ϕ for TM 6 over the course of 10 ns full-solvent dynamics.

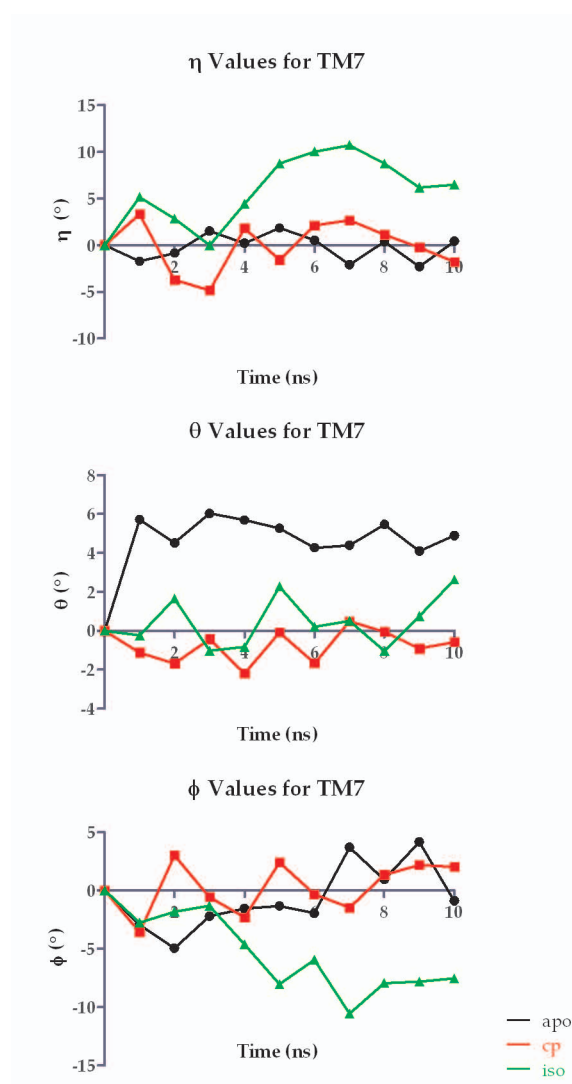


Figure 3.17: Changes to η , θ , and ϕ for TM 7 over the course of 10 ns full-solvent dynamics.

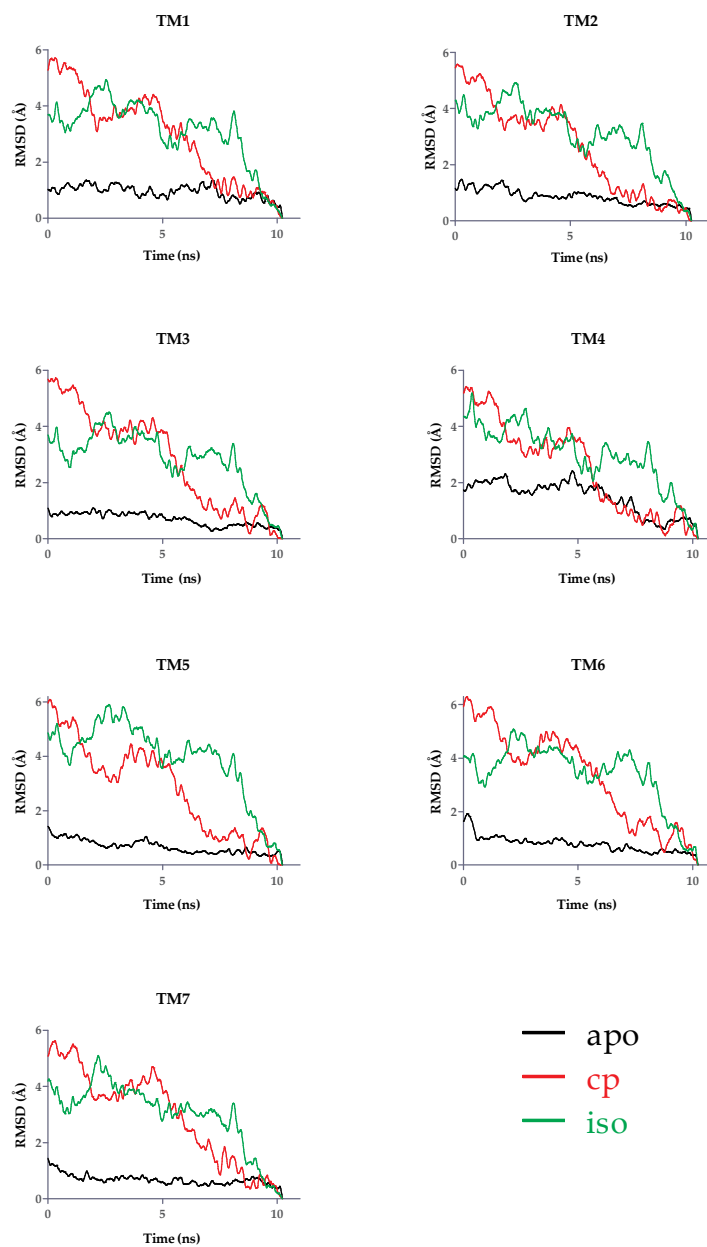


Figure 3.18: TM helix RMSD for apo (black), isoproterenol-bound (green), and cyanopindolol-bound (red) turkey $\beta 1$ shown for each helix individually.